# Precipitation Fluctuation over Semiarid Region in Northern China and the Relationship with El Niño/Southern Oscillation

WEI-CHYUNG WANG

*Atmospheric and Environmental Research Inc., Cambridge, Massachusetts*

KERANG LI

*Institute of Geography, Chinese Academy of Sciences, Beijing, China*

(Manuscript received 30 January 1989, in final form 18 January 1990)

ABSTRACT

In recent years the semiarid region of northern China, which has total annual precipitation between 200 and 500 mm, has shown signs of severe desertification. Intensive theoretical and observational studies are currently underway to examine the climate changes and other contributing factors. In this study, we used the 1951–86 monthly precipitation measurements in this region to study their fluctuations and relationship with the El Niño/Southern Oscillation. Three main features are identified: 1) a 2–3 year quasi-periodic fluctuation, 2) a tendency for rainfall deficiency for the whole region during ENSO years, and 3) a significant correlation between the precipitation fluctuation in the southern part of this region and Southern Oscillation index, with the former lagging the latter by 2–5 months. These features are also evident from analysis of the proxy data during the last hundred years. Discussions on the possible link between the precipitation fluctuation, the summer monsoon, the western Pacific subtropical high, and ENSO are also presented.

## 1. Introduction

Many observational studies in recent years suggest that interannual variations in rainfall at low latitudes, sometimes even at middle and high latitudes, are related to the El Niño (EN) and Southern Oscillation (SO) events in the tropics (Rasmusson and Carpenter 1982, 1983; Rasmusson and Wallace 1983; Ropelewski and Halpert 1987; Weare 1987; Bradley et al. 1987). These EN and SO events are the observed large-scale exchange of mass between the eastern and western hemispheres in the tropical ocean and atmosphere, respectively. The interaction between atmosphere and ocean caused by such exchange will have a profound effect on the global climate. Intensive observational and theoretical studies are underway to understand these ENSO events and their subsequent climatic consequences (see Bradley et al. 1987; Graham and White 1988).

There were many studies concerning the importance of ENSO to climate in China (Fu and Li 1978; Li and Chen 1979, 1980; Wang and Zhao 1981; Guo 1987). These studies have revealed that there exists a long-term coupled oscillation between the equatorial eastern Pacific sea surface temperature (SST) and the location and intensity of the western Pacific subtropical high pressure system. The latter is known to greatly affect the rainfall in eastern China. Li and Sha (1981) have used the tropical Pacific SST to successfully predict the intensity and location of the subtropical high and rainfall belt in eastern China. Thus it appears that there is a strong link between the tropical SST anomalies, subtropical high variations and precipitation fluctuation in eastern China. More discussion are presented in section 4.

In the present study, we investigate the precipitation fluctuation in the semiarid region of northern China, which in recent years has shown a trend toward drier and warmer climate. Identifying these fluctuations and their relations to large scale circulation may lead to a better understanding of the climate trend in this region. We describe in section 2 the geophysical location of the semiarid region and study the spatial and temporal precipitation characteristics. Section 3 presents the cross-spectrum analysis between the precipitation and ENSO to examine their associations. In section 4 we discuss the plausible physical mechanisms for such associations.

## 2. Precipitation characteristics over the semiarid region

The annual mean precipitation over China is about 630 mm. Its distribution (see Fig. 1) shows a decrease

*Corresponding author address:* Dr. Wei-Chyung Wang, Atmospheric Sciences Research Center, State University of New York at Albany, 100 Fuller Road, Albany, NY 12205.

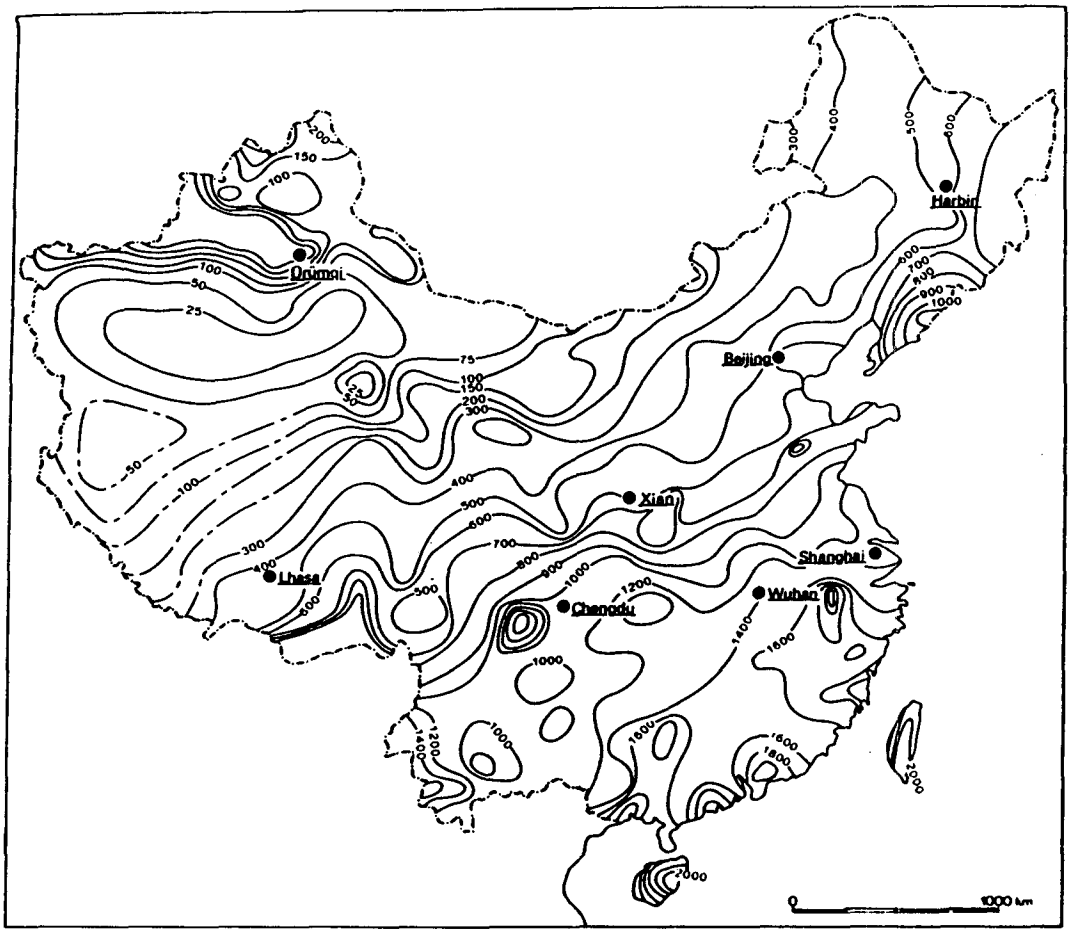


FIG. 1. Annual mean total precipitation (mm) in China (after Domrös and Peng 1988).

from about 2000 mm in the southeastern coastal zones to less than 200 mm in the northwestern inland areas. In general China can be divided into three precipitation regions: the eastern monsoon region, the northwestern arid/semiarid region, and the southwestern plateau region (see Domrös and Peng 1988). The annual precipitation in the arid/semiarid region varies from 25 to 500 mm, with values less than 25 mm in the deserts.

### *a. Semiarid region*

The physical domain of the semiarid region in the present study is defined by performing an empirical orthogonal function analysis of the 1954–86 annual total precipitation measurements at 27 stations in the arid/semiarid region of northern China. Figure 2 shows the station network and the first eigenvector, which accounts for 41% of the total variance. The analysis indicates that there are two distinct, negatively correlated precipitation regions. The first area, covering the middle and western part of the region, has a total annual precipitation of less than 200 mm and the second (mainly in the east) has annual precipitation between 200 and 500 mm. In this study, we concentrate on the second region, which covers the semiarid region in northern China and part of the loess plateau. Because the rainfall in this region is sensitive to the location, timing, and intensity of monsoon, the precipitation exhibits large year-to-year variation. In addition, in recent years this region has shown signs of severe desertification (Zhu and Liu 1983), a feature currently under intensive study; for example, in the Heihe (near station 13 Xining in Fig. 2) experiment to study the atmosphere–land surface processes (Duzheng Ye 1989, personal communication).

### *b. Precipitation fluctuation*

The precipitation in the semiarid region is strongly influenced by the summer monsoon, which accounts for about three-quarters of the total annual precipitation. Consequently, the interannual variability (ratio of standard deviation to mean annual total) which has values between 20% and 30%, largely depends on the summer monsoon variation. To analyze the precipitation fluctuation in this region, we have selected 17

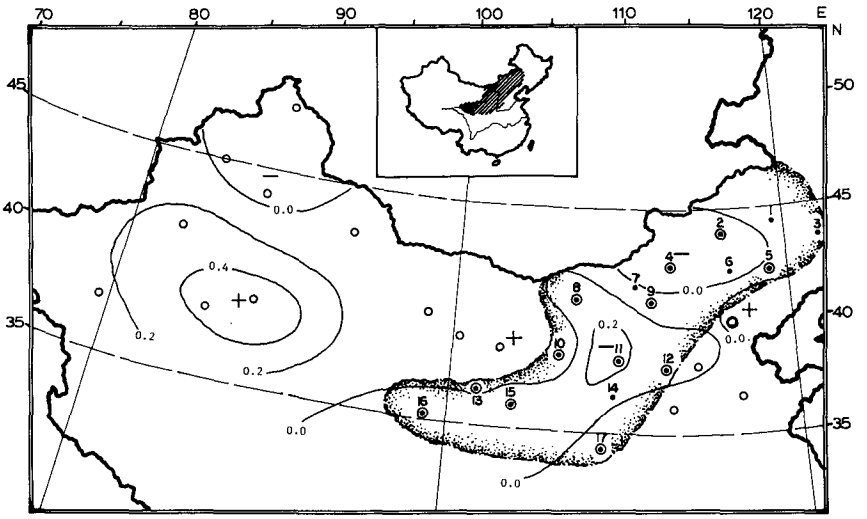


FIG. 2. The first eigenvector of the empirical orthogonal function of 1954–86 annual precipitation anomaly for arid/semiarid region of northern China. Twenty-seven stations, denoted by circles, are used. The stippled-circled region is the semiarid region where the numbered stations (with black dots) are those in which monthly precipitation measurements are used to analyze the precipitation fluctuations.

representative stations (see Table 1 and Fig. 2) with monthly precipitation between 1951–86. Figure 3 shows the time series of the monthly mean precipitation anomaly for six stations—Lindong, Shamba, Hohhot, Yinchuan, Yulin, and Lanzhou. These stations provide a good spatial coverage of the region. After eliminating the short-term fluctuations with a six-month running mean filter, the precipitation anomalies, especially those below normal precipitation, seem to exhibit spatial coherence and persist for many years.

TABLE 1. Stations used in the present study of precipitation fluctuations (see Fig. 2 for station network). All stations have 1951–86 monthly precipitation measurements except Xining and Lindong where no data were taken at 1951–53 and 1951–52, respectively. The stations (except No. 1, 3, 4, and 16) also have proxy dryness/wetness index for 1877–1979 (SMA 1981).

| No. | WMO number | Station | Latitude (°, 'N) | Longitude (°, 'E) | Height (m) |
|---|---|---|---|---|---|
| 1*† | 54027 | Lindong | 44, 00 | 119, 12 | 483 |
| 2 | 54102 | Xilinhot | 43, 57 | 116, 04 | 990 |
| 3 | 54135 | Tongliao | 43, 36 | 122, 16 | 179 |
| 4 | 53276 | Ondor Sum | 42, 24 | 113, 00 | 1150 |
| 5 | 54218 | Chifeng | 42, 16 | 118, 58 | 571 |
| 6 | 54208 | Duolun | 42, 11 | 116, 28 | 1245 |
| 7 | 53352 | Bailingmiao | 41, 42 | 110, 26 | 1376 |
| 8* | 53513 | Shamba | 40, 54 | 107, 06 | 1039 |
| 9*† | 53463 | Hohhot | 40, 49 | 111, 41 | 1063 |
| 10* | 53614 | Yinchuan | 38, 29 | 106, 13 | 1112 |
| 11*† | 53646 | Yulin | 38, 14 | 109, 42 | 1050 |
| 12 | 53772 | Taiyuan | 37, 47 | 112, 33 | 778 |
| 13 | 52866 | Xining | 36, 37 | 101, 46 | 2261 |
| 14 | 53845 | Yan'an | 36, 36 | 109, 30 | 958 |
| 15*† | 52889 | Lanzhou | 36, 03 | 103, 55 | 1517 |
| 16 | 56033 | Madoi | 34, 55 | 98, 13 | 4272 |
| 17 | 57036 | Xian | 34, 18 | 108, 56 | 397 |

* Monthly mean precipitation anomaly is shown in Fig. 3.
† The power spectrum is shown in Fig. 4 and the cross-correlation spectrum is shown in Fig. 6.

Using these monthly precipitation data, we have performed a power-spectrum analysis for the 17 stations. The power spectrum was generated using the methods of Mitchell (1971) and Huang and Li (1984). The maximum lag was set at 144 months. A red (or white) noise "null" continuum was used if the lag-one autocorrelation coefficient, $r_1$, was larger (or equal/smaller) than a critical value $r_c = [-1 + t(n-2)^{1/2}]/(n-1)$, where $n$ is the number of data points and $t = 1.645$ at the 5% level of significance. Since all stations have similar features, we show in Fig. 4 only the spectra for Hohhot, Yulin, Lanzhou, and Lindong. The power spectra for Lindong, Lanzhou, and Hohhot are red noise, and for Yulin white noise.

The power spectrum at Hohhot (Fig. 4a) shows peaks at 32, 8.7, 5.1, and 2.1 months, all significant at 95% confidence level. The maximum peak at Yulin (Fig. 4b) occurs at 18 months with several others at 36, 32, 19.2, 7.4, and 4.6 months. The spectrum at Lanzhou (Fig. 4c) has three significant peaks at 18, 6.4, and 2.7 months. Other prominent peaks at 96, 36, and 14 months are, however, not statistically significant. The peaks at Lindong (Fig. 4d) occur at shorter periods at 15 and 2.1 months. In general, all station results suggest that there are two dominant periodicities: 2–8 and 18–36 months. The quasi 18–36 months is the most dominant period for the semiarid region especially in the southern part of the region (south of 42°N shown in Fig. 2). This result is consistent with the findings by Wang and Zhao (1981), Xu and Dong (1982), and Clegg and Wigley (1984), who have an-

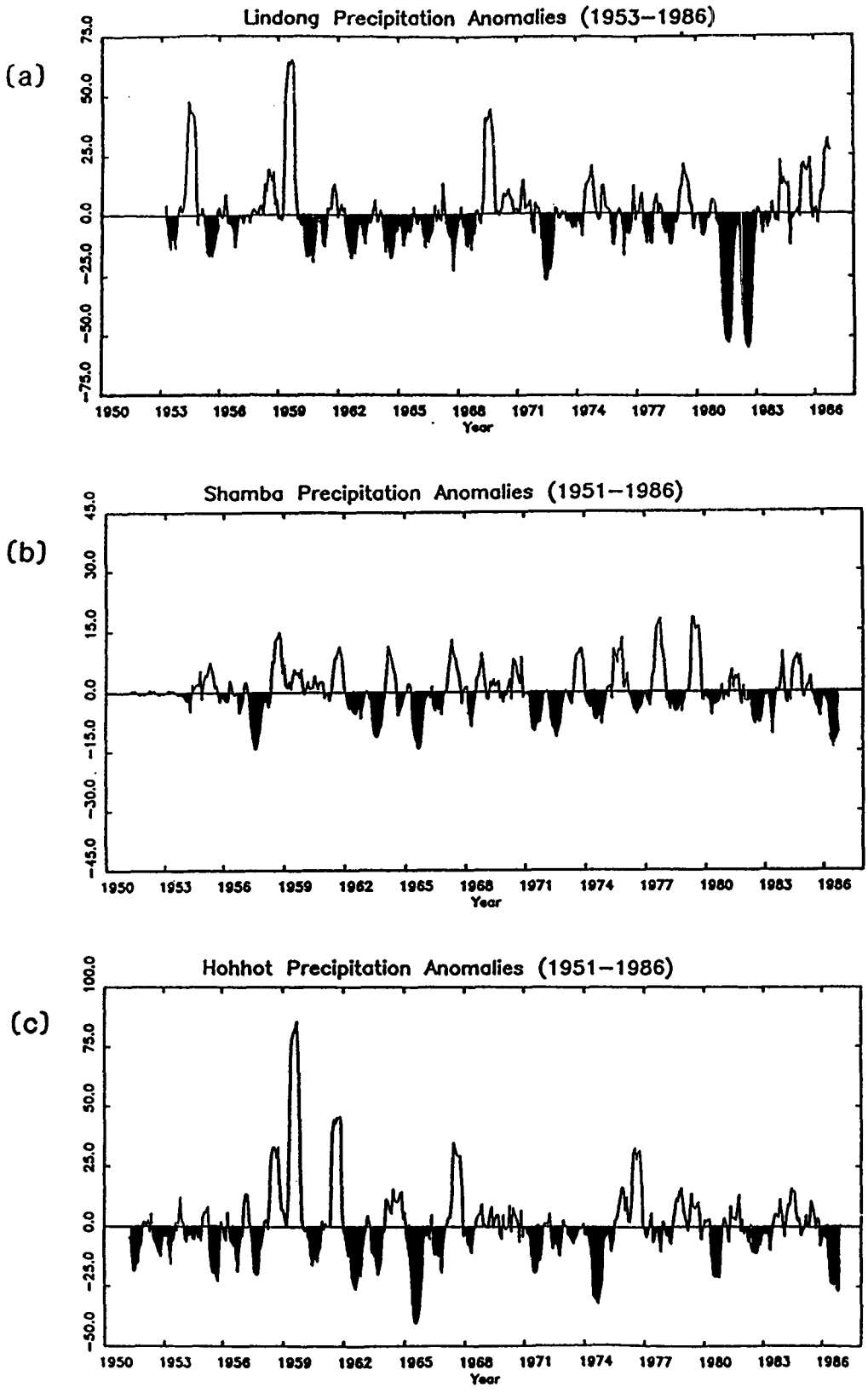


FIG. 3. The 1951–86 monthly precipitation anomaly (mm) at (a) Lindong, (b) Shamba, (c) Hohhot, (d) Yinchuan, (e) Yulin, and (f) Lanzhou. See Table 1 and Fig. 2 for station location.

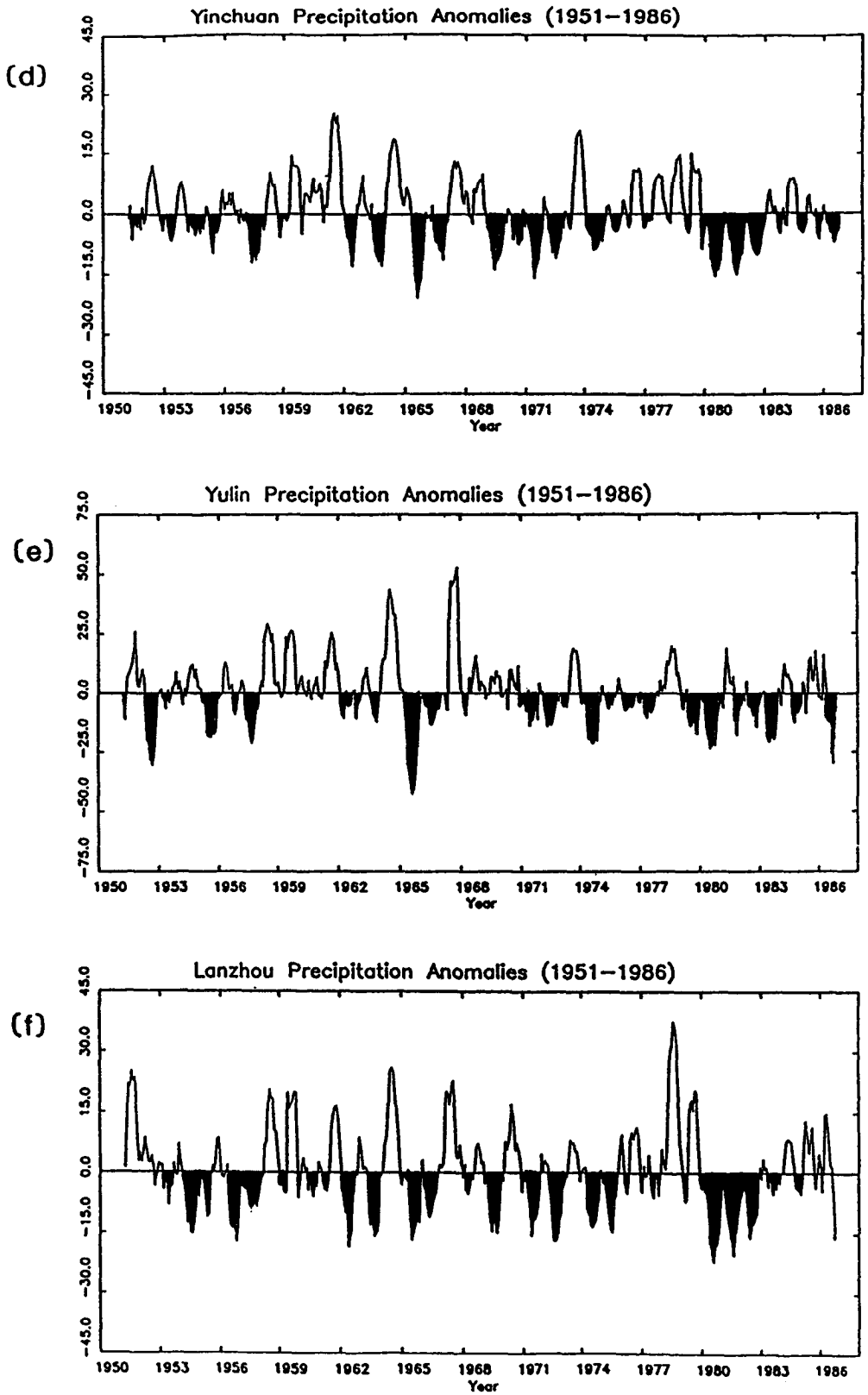


FIG. 3. (*Continued*)

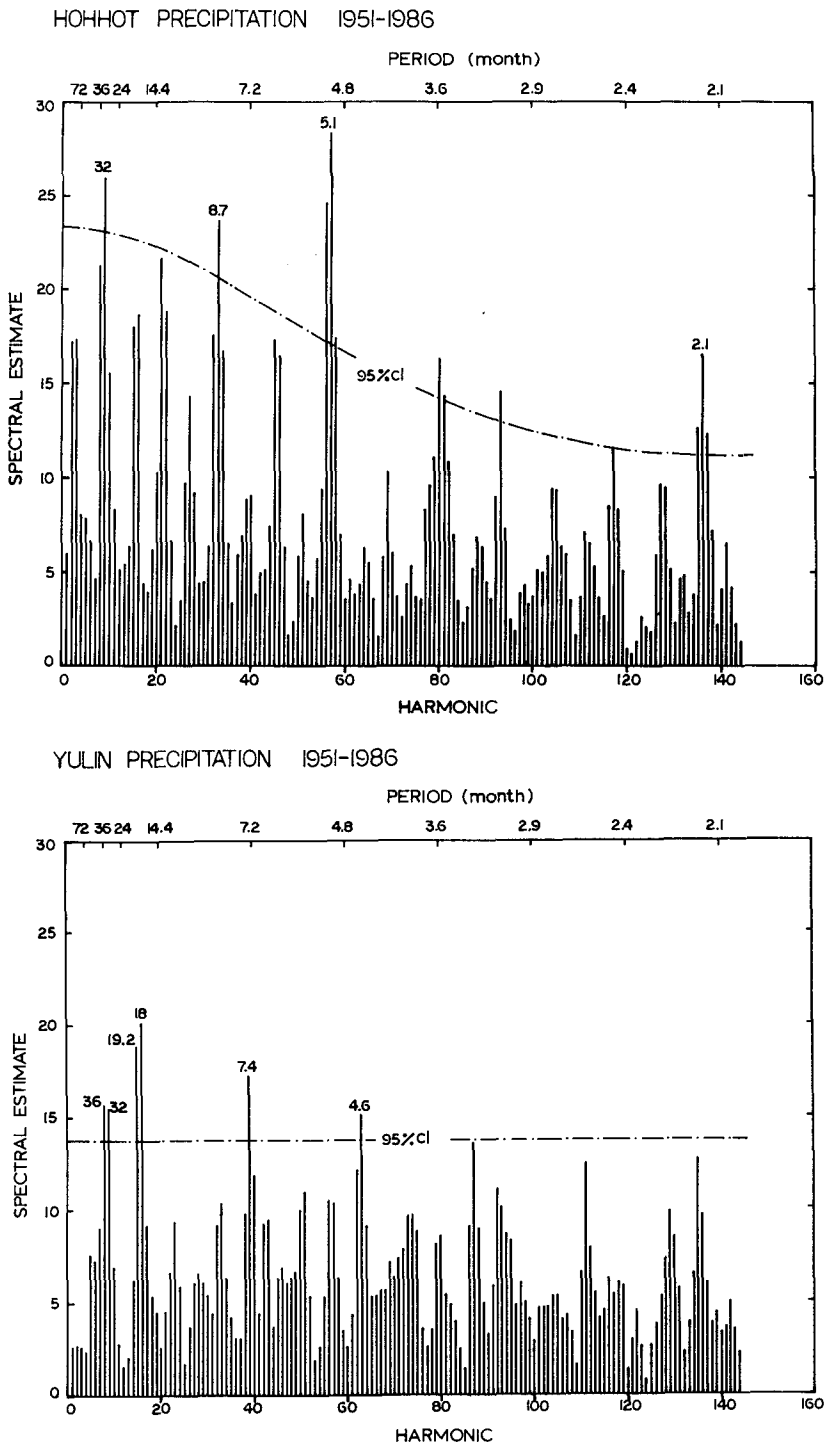


FIG. 4. Power spectrum of 1951–86 precipitation anomaly at (a) Hohhot, (b) Yulin, (c) Lanzhou, and (d) Lindong. Broken line is 95% confidence level and maximum lag is 144 months.

alyzed the precipitation fluctuations over similar areas or neighboring regions that we studied here. Note, however, that the dominant period in the northern part of the semiarid region (north of 42°N) is shorter, about 15 months or less. The different characteristics between the southern and northern parts of the semiarid region

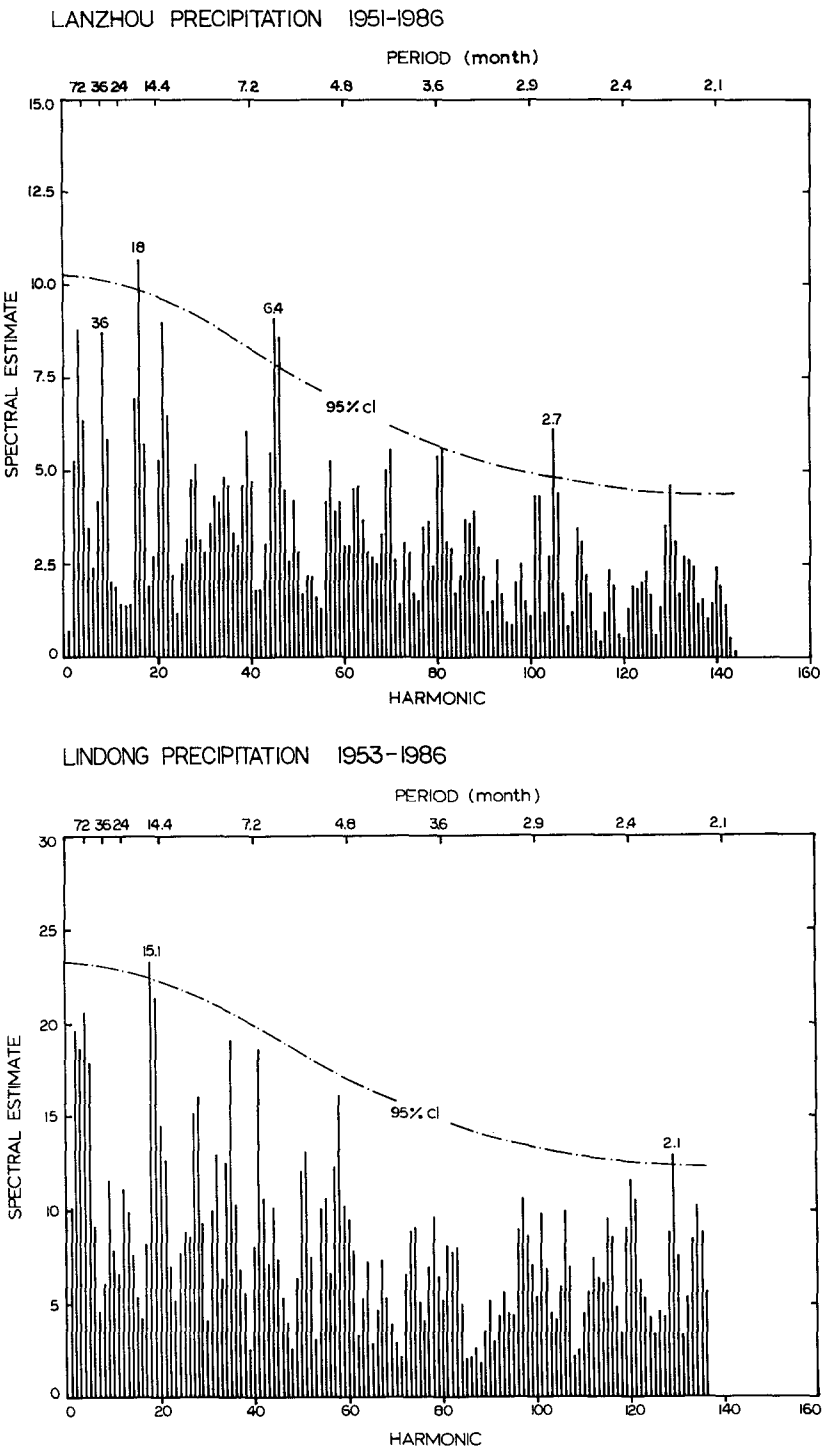


FIG. 4. (*Continued*)

can also be seen in the cross-correlation spectra discussed in section 3.

We have also used the 1950–83 SO index (normalized series of Tahiti–Darwin sea-level pressure) and the SST index (mean anomaly over equatorial central and eastern Pacific; Wright 1984) to calculate the respective power spectrum. Much of the variance in the spectrum is contained in the wavelength bands 2–7 years. As mentioned earlier, similar results were found by Fu and Li (1978) and Li and Sha (1981) when they

TABLE 2. Anomaly of total summer (June–July–August) precipitation (mm) during the El Niño years.*

| No.*† | Station | 1952 | 1953 | 1957 | 1963 | 1965 | 1969 | 1972 | 1976 | 1982 | 1983 | 1986 |
|---|---|---|---|---|---|---|---|---|---|---|---|---|
| 1 | Lindong | — | −61.3 | 7.5 | 3.0 | −2.8 | 266.1 | −157.0 | −23.6 | −267.7 | −33.7 | 77.3 |
| 8 | Shamba | −0.6 | −0.6 | −58.6 | −43.6 | −60.6 | 29.4 | −48.6 | −25.6 | −26.6 | −60.6 | −51.6 |
| 9 | Hohhot | −32.2 | −26.2 | −75.2 | −105.2 | −189.2 | −1.2 | −60.2 | 180.8 | −55.2 | −9.2 | −111.2 |
| 10 | Yinchuan | 41.5 | −18.2 | −56.4 | −37.2 | −91.2 | −58.5 | −23.7 | 87.7 | −42.5 | −31.5 | −12.5 |
| 11 | Yulin | −182.1 | 11.7 | −95.1 | −20.4 | −180.9 | −22.7 | −32.6 | −3.5 | −31.2 | −137.2 | −6.2 |
| 15 | Lanzhou | −9.1 | −24.5 | −13.3 | −91.1 | −69.1 | −90.0 | −44.6 | 71.0 | −73.1 | −7.1 | 33.9 |

* The mean total summer precipitation averaged over the period 1951–1986 is Lindong (284.7), Shamba (88.7), Hohhot (272.3), Yinchuan (114.5), Yulin (244.3) and Lanzhou (178.1).
† Station number marked on Fig. 2.

analyzed the SST of the Pacific Ocean. These suggest there exists a relationship between the ENSO events and the precipitation fluctuation in the semiarid region.

Before we discuss the cross-correlation spectra between the ENSO and precipitation fluctuation, there are three cases that strongly suggest that below normal precipitation was usually associated with intense EN years. The first case is the consistency of the precipitation anomaly among the stations and their close association with EN. The data shown in Table 2 indicate that notable precipitation deficiency years often occurred during the EN years. Note that the driest year in Table 2 for each station is also the driest year for the whole period 1951–86. In addition, it is interesting to note that there is a tendency for larger rainfall to occur during the "cold event" years 1954, 1964, 1970, 1973, and 1975 cited in Bradley et al. (1987). Second, Lanzhou has longer precipitation measurements for 1932–86; Fig. 5 shows the time series with EN years indicated. Note that the rainfalls were below normal in 13 of the 16 EN years. Third, we have used the 1877–79 annual dryness/wetness index (SMA 1981) of the 13 stations in the semiarid region (see Table 1) to examine their characteristics. The results in Table 3 show that 23 of the 33 EN events during the last 100 years (Fu et al. 1986; Quinn et al. 1987) were accompanied by a below normal rainfall in this region. In particular, during very strong EN years 1877, 1878, 1891, 1925, 1926, 1982, and 1983 (see Quinn et al. 1987), more than 65% of the area (except 1925) was in the dry/drought category. Thus these results further substantiate the evidence that below normal rainfall usually occurred during intense EN years. In what follows we investigate to what extent the precipitation fluctuation in the semiarid region is associated with ENSO events.

## 3. Relationship between precipitation and ENSO

Cross-spectrum analysis is a useful method to understand the relationship between two time series (Essenwanger 1986). If a relationship exists between the

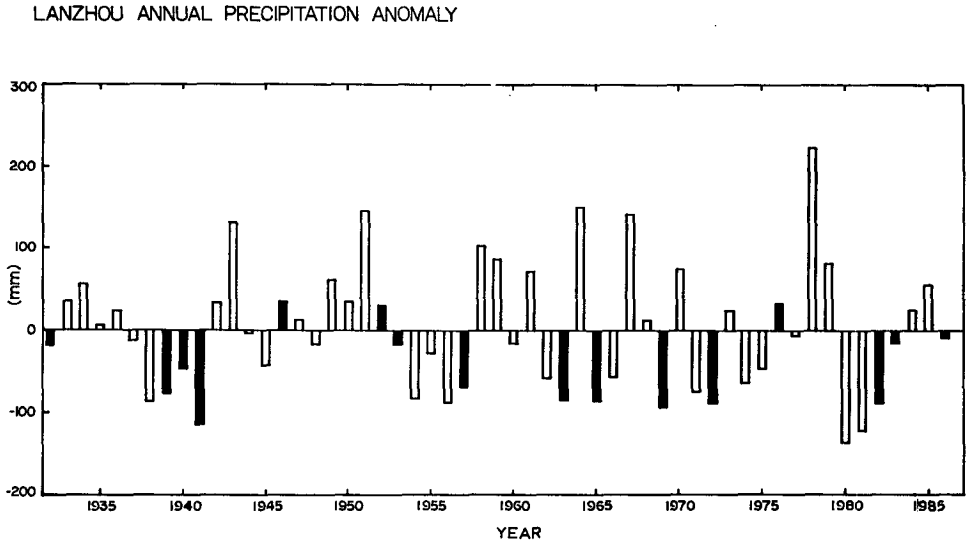


FIG. 5. The 1932–86 annual precipitation anomaly (mm) at Lanzhou. Solid bars are El Niño years.

TABLE 3. Dry/wet area index (in percent) averaged over 13 stations (see Table 1) during EN years for the period 1877 to 1979. The individual station index has been classified into 1, 2, 3, 4 and 5 grades corresponding to flood, wet, normal, dry and drought, respectively (cf. SMA 1981). The dry area index (DAI) is the percent of stations with grades 4 and 5 while wet area index (WAI) with grades 1 and 2. Therefore, the DAI and WAI reflect the fraction of the study region with dry and wet conditions, respectively. Years marked with asterisks are the years with very strong EN intensities (Quinn et al. 1987).

| ENSO year | DAI | WAI |
|---|---|---|
| 1877* | 93 | 0 |
| 1878* | 79 | 7 |
| 1880 | 7 | 36 |
| 1884 | 38 | 31 |
| 1887 | 15 | 54 |
| 1888 | 29 | 21 |
| 1891* | 73 | 20 |
| 1896 | 20 | 47 |
| 1899 | 74 | 13 |
| 1902 | 50 | 12 |
| 1904 | 19 | 75 |
| 1905 | 53 | 34 |
| 1911 | 18 | 29 |
| 1913 | 34 | 33 |
| 1914 | 24 | 47 |
| 1918 | 12 | 29 |
| 1925* | 29 | 24 |
| 1926* | 65 | 11 |
| 1930 | 50 | 22 |
| 1939 | 45 | 33 |
| 1940 | 6 | 76 |
| 1941 | 76 | 6 |
| 1946 | 39 | 44 |
| 1952 | 50 | 22 |
| 1953 | 34 | 22 |
| 1957 | 67 | 11 |
| 1963 | 50 | 22 |
| 1965 | 94 | 0 |
| 1969 | 39 | 22 |
| 1972 | 94 | 0 |
| 1976 | 11 | 50 |
| 1982* | 69 | 23 |
| 1983* | 69 | 15 |

precipitation and the ENSO in the periodicities found in the power-spectrum analysis, the cross-spectrum analysis will reveal whether the relationship is associated with high or low frequencies. On the other hand, if the datasets appear uncorrelated, the analysis will also indicate whether this feature is a result of compensation; for example, between the negative correlation at low frequencies and positive correlation at high frequencies.

Cross-correlation between two time series can be investigated by calculating the cross-spectrum, which includes the co-spectrum, quadrature spectrum, phase spectrum, and coherence spectrum (Huang and Li 1984). Coherence is a measure of the correlation between two variables at each discrete frequency interval. A significance criterion for coherence is the expectancy (Essenwanger 1986)

$$R = [1 - \alpha^{1/(\nu-1)}]^{1/2},$$

where $\nu = 2n/m - 0.5$ stands for the degrees of freedom, $\alpha$ is the probability of significance level, and $n$ and $m$ are the numbers of data points and maximum lag, respectively; here $n = 396$ months and $m = 66$ months. The phase spectrum displays the phase lag relationship of the two time series at different frequency while the cospectrum and quadrature spectrum provide the correlated relationships at the same phase and 90° phase difference.

### *a. Precipitation and SO*

Figure 6 shows the cross-correlation spectra between the SO index and precipitation for the four stations discussed in section 2.2. We concentrate our discussion on the low frequency bands, especially the 2–3 years period.

The results shown in Fig. 6a for Hohhot indicate that the maximum coherence in the low frequency is 0.423, at a corresponding period of 33 months with 0.001 level of significance. Note that peaks also occur at high frequency bands of 2 to 8 months. Cospectrum analysis shows that cross-correlation of these two series at the same phase has positive contribution in the low frequency of 11–33 months. The phase spectrum, shown on the upper panel of the figure, indicates that variation of the SO in the low frequency band with periods of 18.9–44 months generally precedes the precipitation variation by 2–5 months; for example, the lag time for period 33 months is 2.9 months. These results imply that about 3 months after the anomaly of SO changes from positive to negative, the precipitation changes from positive to negative.

The cross-correlation spectra between the SO index and precipitation at Yulin (Fig. 6b) show that there are also pronounced peaks of coherence for fluctuation at low frequency bands 22–44 months and 15–17 months, all significant at the 95% confidence level. The maximum coherence is 0.531 at period 33 months and 0.838 at period 14.7 months, both with 0.001 level of significance. Other peaks exist at high frequency bands 2–5 months. The correlation of these two series at the same phase is positive in the low frequency bands of 19–44 months. The phase spectrum indicates that the variation of the SO in the low frequency bands 19–44 months precedes the precipitation variation by 2–5 months; for example, the lag time corresponding to period 33 months is 3 months. The cross-correlation spectra between the SO index and precipitation at Lanzhou (Fig. 6c) have similar features in low frequencies as found at Hohhot and Yulin. The lag time corresponding to period 33 months is 2.7 months. Although other stations located south of 42°N in Fig. 2 show similar features as those in Hohhot, Yulin, and

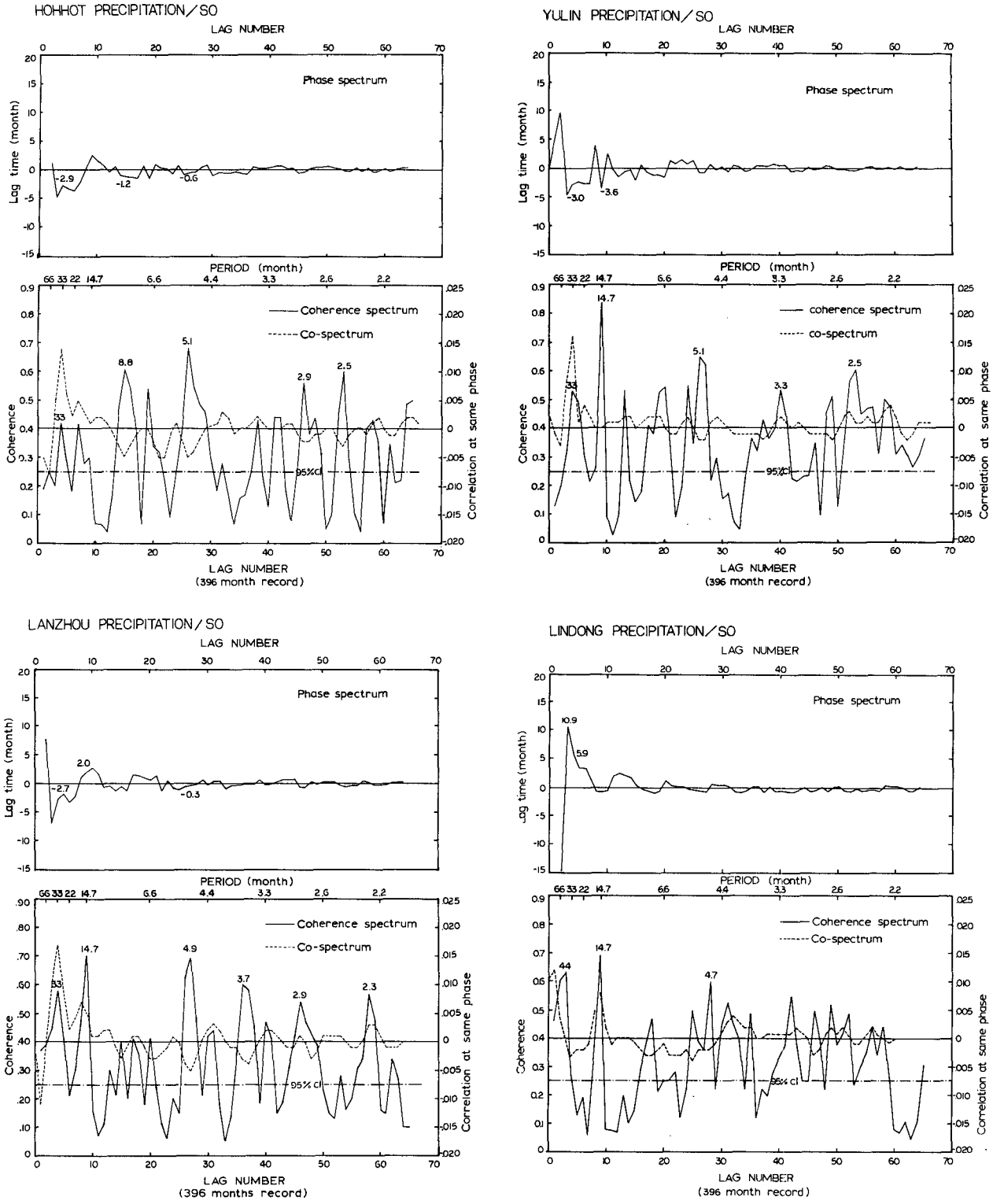


FIG. 6. The cross-spectrum analysis between the Southern Oscillation (SO) Index and precipitation at (a) Hohhot, (b) Yulin, (c) Lanzhou, and (d) Lindong for 1951–83. Broken line is 95% confidence level and maximum lag is 66 months. Positive lag time means that precipitation leads SO.

Lanzhou, the stations in the north show different characteristics as represented by Lindong (Fig. 6d). The cospectrum shows that the SO and precipitation have a negative contribution in the low frequency bands 19–44 months. In addition, the SO lags the precipitation fluctuation by 2–11 months.

In summary, the analyses suggest there exist pronounced peaks of coherence between the SO and precipitation fluctuation in the frequency bands 2–3 years in the semiarid region. However, the phase-spectrum and cospectrum analyses show that there are two distinct subregions with different cross-correlation characteristics. In the subregion south of 42°N, the variation of the SO with quasi periods of 2 to 3 years has positive correlation with the precipitation fluctuation and precedes the precipitation fluctuation by 2–5 months. In the second subregion located north of 42°N, the SO has negative correlation with the precipitation fluctuation and lags the fluctuation by up to 10 months. These features can be clearly seen in Table 4, which summarizes the lag time corresponding to 33 months for all the stations in the semiarid region. These results indicate that the SO plays a more important role in the precipitation fluctuation in the areas south of 42°N of the semiarid region than in the north. This difference in characteristics between the southern and northern part of the semiarid region also reflects the extreme northern limit of the summer monsoon (see discussion in section 4).

### *b. Precipitation and EN*

We have also performed the cross-spectrum analysis between the precipitation and the SST index. Figure 7 shows the spectra for the same four stations discussed in section 3.1. The pronounced peaks of coherence at Hohhot (Fig. 7a) are found at periods 25–66 months, all at 95% confidence level. The peaks of coherence in the low frequency are 0.451 at period 33 months and 0.481 at period 18.9 months, both with 0.001 significance level. However, the cospectrum analysis shows that the cross-correlation of these two series have negative contribution in the low frequency bands 15–44 months. The phase-spectrum indicates that the variation of EN in the low frequency generally precedes the precipitation variation by 2–5 months; for example, the lag time corresponding to 33 months is 2.9 months.

Figure 7b shows the cross-spectrum analysis between SST index and precipitation at Yulin. The pronounced peaks in the low frequency bands correspond to periods 15–44 months, significance at 95% confidence level. The maximum coherence is 0.682, corresponding to a period 14.7 months with 0.001 significance level. The next peak of 0.642 corresponds to a period 33 months, also with 0.001 significance level. The cross correlation of the two series at the same phase has a negative contribution in the low frequency bands 15–33 months. The variation of the SST index in the low frequency bands 19–44 months precedes the precipitation variation by 2 to 3 months; for example, the lag time corresponding to period 33 months is 2.7 months. For Lanzhou (Fig. 7c), similar features are found in the low frequency bands 15–44 months. The lag time corresponding to period 33 months is 2.3 months. However, Lindong (Fig. 7d) shows different characteristics, a feature observed already in the results found between the SO and precipitation discussed in section 3.1. The phase spectrum shows different responses when compared with the stations south of 42°N. The cospectrum analysis suggests there is a positive contribution in the low frequency bands 19–44 months between the EN and precipitation fluctuation with the former lagging the latter by 1–11 months.

These results suggest that, between the EN and precipitation fluctuation, there also exist pronounced peaks of coherence with quasi-periods 2–3 years, and that within the semiarid region, there are two subregions with different characteristics. As summarized in Table 4, the EN with a period 33 months precedes the precipitation fluctuation by 2–5 months in the southern region but lags by up to 11 months in the northern region. This feature is consistent with the findings between the SO and precipitation fluctuation mentioned earlier.

TABLE 4. The lag time (months)* corresponding to period 33 months between ENSO and precipitation.

| No. | Station | Latitude (°, 'N) | SO | EN |
|---|---|---|---|---|
| 1 | Lindong | 44, 00 | 10.9 | 10.6 |
| 2 | Xilinhot | 43, 57 | 2.6 | 2.1 |
| 3 | Tongliao | 43, 36 | 8.2 | 0.9 |
| 4 | Ondor Sum | 42, 24 | 0.9 | 0.9 |
| 5 | Chifeng | 42, 16 | −4.4 | 0.1 |
| 6 | Duolun | 42, 11 | −2.9 | −4.2 |
| 7 | Bailingmiao | 41, 42 | −1.3 | −2.4 |
| 8 | Shamba | 40, 54 | −5.0 | −5.0 |
| 9 | Hohhot | 40, 49 | −2.9 | −2.9 |
| 10 | Yinchuan | 38, 29 | −2.0 | −2.4 |
| 11 | Yulin | 38, 14 | −3.0 | −2.7 |
| 12 | Taiyuan | 37, 47 | −0.5 | −4.5 |
| 13 | Xining | 36, 37 | −2.3 | −2.3 |
| 14 | Yan'an | 36, 36 | −3.1 | −3.6 |
| 15 | Lanzhou | 36, 03 | −2.7 | −2.3 |
| 16 | Madoi | 34, 55 | −2.0 | −1.1 |
| 17 | Xian | 34, 18 | −2.1 | −2.3 |

* Positive/negative values mean that the variation of SO (or EN) succeeds/precedes the variation of precipitation.

## 4. Discussion and conclusion

The results presented above suggest there exists a significant correlation between the monthly precipitation in semiarid region of northern China and ENSO in the frequency bands 2–3 years. The results further

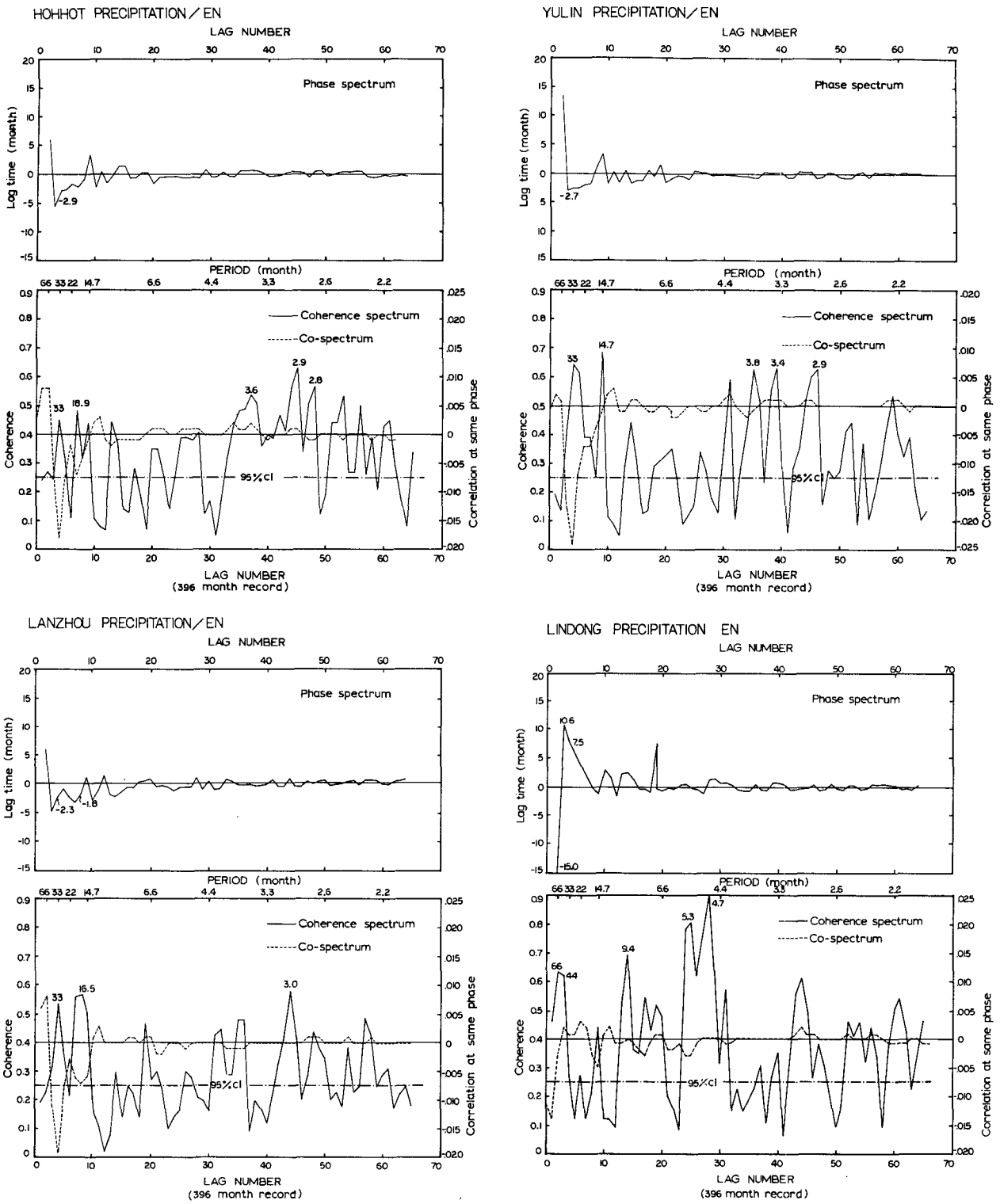


FIG. 7. Same as in Fig. 6 except between sea surface temperature (SST) index and precipitation.

indicate that during ENSO years rainfall was usually below normal and drought sometimes occurred. However, cross-spectrum analysis reveals that, within the semiarid region, the phase of the correlation is different in the northern part (north of 42°N) than in the southern part. For example, ENSO with a period 33 months precedes the precipitation fluctuation by 2–5 months in the southern part of the semiarid region, but lags up to 11 months in the northern part. As discussed below, the close correlation between the precipitation fluctuation and ENSO can be explained by the coupling processes involving the summer monsoon and the western Pacific subtropical high.

It is known that the summer monsoon is the major source of precipitation in China (see Domrös and Peng 1988). Thus, there is a close correlation between the rainy season and the period of onset and withdrawal of the monsoon. It is also known that the northward movement of the rainfall belt in eastern China during the period May through September has gone through two jumps and three stable periods (see Fig. 8; Xu et al. 1983). (Here, the rainfall belt is defined as the isohyet of the maximum rainfall averaged over 10 days.) For a month after the middle of May, the rainfall belt moves between 23°–25°N over southern China. However, within 10 days after the middle of June it advances rapidly northward 6 to 7 degrees and reaches the middle and lower Changjiang (Yangtze River) valley. For the next few weeks the rainfall belt stays between 30°–35°N. In the middle of July it jumps northward again and reaches its extreme northern latitudes in early August. Shortly thereafter, the rainfall belt starts to move southward.

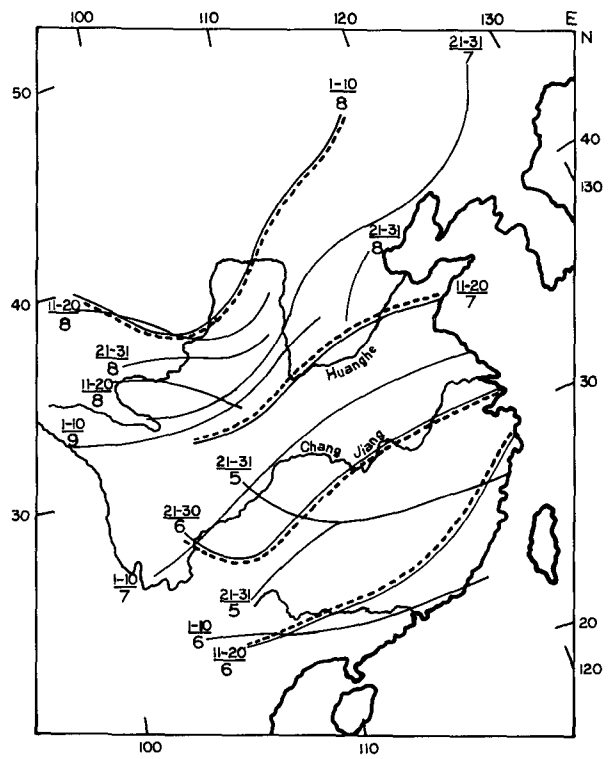


FIG. 8. The latitudinal movement of the rainfall belt in eastern China. The denominator is the month and the numerator the date (after Xu et al. 1983). The starting and ending dates of the two jumps are 11–20 June and 21–30 June, and 11–20 July and 1–10 August; both are marked with dashed lines.

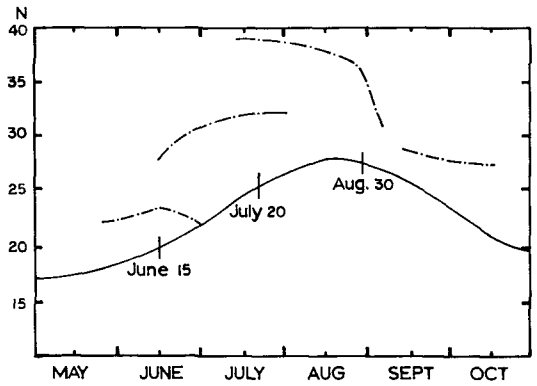


FIG. 9. The location of ridge lines of the western Pacific subtropical high at 500 mb (solid line; averaged over 110°–150°E) and the maximum rainfall belt (dot-dashed line; averaged over 110°–120°E) (after GDBU 1971).

In addition, the advance of the summer monsoon (thus the rainfall belt) has a close connection with the northward migration of the western Pacific subtropical high (GDBU 1971; Domrös and Peng 1988). The rainfall belt lies about 8–9 degrees of latitude to the north of the subtropical high ridge (see Fig. 9). The subtropical high moves northwest and strengthens from winter to summer, and vice versa. It also possesses two sudden jumps and three stable periods, which coincide with the timings of the latitudinal movement of the rainfall belt. Therefore, the location of the rainfall belt is directly related to the location of the western Pacific subtropical high. For example, when the western Pacific subtropical high moves further west, it will tend to decrease the extent of the northward movement of the rainfall belt, and result in a decrease of rainfall in the semiarid region.

Studies by Fu and Li (1978) and Li and Chen (1979) have shown that the western Pacific subtropical high is influenced by the SST of the equatorial eastern Pacific ocean. The SST and the intensity of the subtropical high are positively correlated; both have a quasi-period of 3 years oscillation where the SST anomaly leads the variation of the intensity by 6 months. The SST also affects the location of the subtropical high. For example, when equatorial eastern Pacific SST warms (more than normal) in winter during EN years, the location of the subtropical high shifts westward in next summer.

TABLE 5. Coupling processes linking the SST in equatorial eastern Pacific Ocean, the western Pacific subtropical high, and the precipitation of semiarid region in northern China.

| Climate feature | Variation |
|---|---|
| • SST in equatorial eastern Pacific Ocean | Warmer during EN years |
| • Intensity of Hadley circulation | Increase |
| • Western Pacific subtropical high | |
| —Location | Westward |
| —Intensity | Increase |
| • Northern limit of summer monsoon | Southward |
| • Precipitation of semiarid region in northern China | Decrease |

The physical mechanisms linking the western Pacific subtropical high and SST in the equatorial eastern Pacific ocean have been discussed in detail in Fu and Zhao (1979), Fu and Su (1981), Fu et al. (1986), and Ye (1987) and are briefly summarized here. When SST in the equatorial eastern Pacific becomes warmer during EN years, the meridional temperature gradient will become larger, thus implying a stronger Hadley cell. A stronger Hadley circulation will induce a stronger intensity of the western Pacific subtropical high, which together with a westward shift of the location of the subtropical high can lead to a decrease in the extent of the northern latitude of the summer monsoon and result in a decrease of the precipitation in the semiarid region. In summary, as shown in Table 5 the variation of the SST, through interactions with the meridional circulation, will affect the subtropical high, which in turn will affect the summer monsoon and thus precipitation over semiarid region in northern China.

Finally, it is worthwhile to discuss why there is a phase difference in the correlation for the northern and southern parts of the semiarid region. As shown in Fig. 9, the extreme northern latitude of the maximum rainfall belt reaches around 40°N. This implies that the northern part of the semiarid region is subject less to the influence of the summer monsoon than the southern part. Indeed, we have recently performed the complex empirical orthogonal function analysis to study the spatial phase of the rainfall propagation during summer for the whole of China. Preliminary results indicate that the northern part of the semiarid region also receives the moisture from the west, which provides different rainfall characteristics than the summer monsoon. Details of the study are included in a separate paper (under preparation).

*Acknowledgments.* We thank Congbin Fu, Shiyuan Tao, Zuzheng Ye, and D. Gutzler for comments on the manuscript. We would also like to thank the two anonymous reviewers whose constructive comments and suggestions greatly clarified the manuscript. Kerang Li participated in the study as a visiting scholar under the United States' Department of Energy and the People's Republic of China's Chinese Academy of Science Joint Research on the Greenhouse Effect. The work was supported by a grant from the Atmospheric and Climate Division, Office of Health and Environmental Sciences, Department of Energy (DE-FG02-86-ER60422).

## REFERENCES

Bradley, R. S., H. F. Diaz, G. N. Kiladis and J. K. Eischeid, 1987: ENSO signal in continental temperature and precipitation records. *Nature,* **327,** 497–501.

Clegg, S. S., and T. M. Wigley, 1984: Periodicities in precipitation in Northeast China, 1470–1979. *Geophys. Res. Lett.*, **11,** 1219–1222.

Domrös, M., and G. Peng, 1988: *The Climate of China.* Springer-Verlag, 360 pp.

Essenwanger, O. M., 1986: Elements of statistical analysis, *General Climatology.* Elsevier 424 pp.

Fu, C., and K. R. Li, 1978: The effects of tropical ocean on the western Pacific subtropical high. *Oceanic Selections,* No. 2, Ocean Press, 16–21.

——, and Y. F. Zhao, 1979: The sea temperature in equatorial Pacific and vertical circulation cell of atmosphere. *Scientia Atmospherica Sinica,* **3,** 50–57, (in Chinese).

——, and B. K. Su, 1981: The long-term fluctuation of sea-surface temperature in main currents of the North Pacific Ocean. *Oceanologia et Limnologia Sinica Suppl.,* Ocean Press, 29–40, (in Chinese).

——, H. F. Diaz and J. O. Fletcher, 1986: Characteristics of the response of sea surface temperature in the Central Pacific associated with warm episodes of the Southern Oscillation. *Mon. Wea. Rev.*, **114,** 1716–1738.

GDBU (Geophysical Department, Beijing University), 1971: *Atmospheric Circulation and Medium-Range Weather Process.* Beijing University, 250 pp., (in Chinese).

Graham, N. E., and W. B. White, 1988: The El Niño cycle: A natural oscillator of the Pacific Ocean-atmosphere system. *Science,* **240,** 1293–1302.

Guo, Q., 1987: The east Asia monsoon and the Southern Oscillation, 1871–1980, *The Climate of China and Global Climate,* Ocean Press, 249–255.

Huang, J., and H. Li, 1984: *Power Spectrum Analysis Used in Meteorology.* Meteorology Press, 318 pp., (in Chinese).

Li, K.-R., and Y. S. Chen, 1979: Some facts about the effect of the meridional difference of SST anomalies of north Pacific on the subtropical high. *Scientia Atmospherica Sinica,* **3**(2), (in Chinese).

——, and ——, 1980: An analysis of the space–time characteristics of the SST field in the North Pacific., *Oceanologia et Limnologia Sinica,* **2**(3), (in Chinese).

——, and W. Sha, 1981: The application of SST to the long-term forecasting of subtropical high and rain-belt. *Collected Works in Medium- and Long-Range Forecast.* Office of Chang Jiang River Valley, 351 pp., (in Chinese).

Mitchell, J. M., 1971: Climatic change. World Meteorological Organization, No. 195, TP 100.

Quinn, W. H., V. T. Neal and S. E. Antunez de Mayolo, 1987: El Niño occurrences over the four and a half centuries. *J. Geophys. Res.*, **92,** 14449–14461.

Rasmusson, E. M., and T. H. Carpenter, 1982: Variations in tropical sea surface temperature and surface wind fields associated with

the Southern Oscillation/El Niño. *Mon. Wea. Rev.*, **110,** 354–384.

——, and ——, 1983: The relationship between eastern equatorial Pacific sea surface temperatures and rainfall over India and Sri Lanka. *Mon. Wea. Rev.*, **111,** 517–528.

——, and J. M. Wallace, 1983: Meteorological aspects of the El Niño/Southern Oscillation. *Science,* **222,** 1195–1202.

Ropelewski, C. F., and M. S. Halpert, 1987: Global and regional scale precipitation patterns associated with the El Niño/Southern Oscillation. *Mon. Wea. Rev.*, **115,** 1606–1626.

SMA (State Meteorological Administration), 1981: *Yearly Charts of Dryness/Wetness in China for the Last 500 Year Period.* Atlas Press, 332 pp.

Wang, S.-W., and Z.-C. Zhao, 1981: Droughts and floods in China, 1470–1979, *Climate and History,* Wigley, et al, Eds. Cambridge University Press, 271–288.

Weare, B. C., 1987: Relationships between monthly precipitation and SST variations in the tropical Pacific region. *Mon. Wea. Rev.*, **115,** 2687–2698.

Wright, P. B., 1984: Relationships between indices of the Southern Oscillation. *Mon. Wea. Rev.*, **112,** 1913–1919.

Xu, G., and A. Dong, 1982: The quasi-three year period of precipitation in the west of China. *Plateau Meteorology,* **1**(2), (in Chinese).

——, and M. Li and Z. Zhang, 1983: Seasonal variation of the rainbelts in China. *Scientia Atmospherica Sinica,* 7(3), (in Chinese).

Ye, D., 1987: Some aspects of low-frequency phenomena of the air–sea interaction—a review of the recent advances. *The Climate of China and Global Climate,* Ocean Press, 154–156.

Zhu, Z., and S. Liu, 1983: *Combatting Desertification in Arid and Semiarid Zones in China.* Institute of Desert Research, Academia Sinica, 69 pp.